ResearchGate

See discussions, stats, and author profiles for this publication at: https://www.researchgate.net/publication/263940760

Low-Temperature Synthesis of Copper(II) Sulfide Quantum Dot Decorated TiO2 Nanotubes and Their Photocatalytic Properties

ARTICLE *in* THE JOURNAL OF PHYSICAL CHEMISTRY C · MARCH 2011

Impact Factor: 4.77 · DOI: 10.1021/jp109716q

CITATIONS
35

READS
128

4 AUTHORS, INCLUDING:

Chalita Ratanatawanate
National Nanotechnology Center, Thailand
15 PUBLICATIONS **388** CITATIONS
SEE PROFILE

Khiem Vu
University of Texas Southwestern Medical C…
3 PUBLICATIONS **232** CITATIONS
SEE PROFILE

K. J. Balkus
University of Texas at Dallas
238 PUBLICATIONS **5,855** CITATIONS
SEE PROFILE

Available from: Khiem Vu
Retrieved on: 02 February 2016

THE JOURNAL OF PHYSICAL CHEMISTRY C

ARTICLE

pubs.acs.org/JPCC

Low-Temperature Synthesis of Copper(II) Sulfide Quantum Dot Decorated TiO_2 Nanotubes and Their Photocatalytic Properties

Chalita Ratanatawanate, Amanda Bui, Khiem Vu, and Kenneth J. Balkus, Jr.*

The University of Texas at Dallas, Department of Chemistry and the Alan G. MacDiarmid NanoTech Institute, 800 West Campbell Road, Richardson, Texas 75080-3021, United States

ABSTRACT: TiO_2 nanotubes functionalized with copper sulfide quantum dots were successfully prepared by a stepwise crystallization of CuS nanoparticles onto the nanotubes, using cysteine linkers. The products were characterized by Fourier transform infrared spectroscopy (FT-IR), X-ray diffraction (XRD), transmission electron microscopy (TEM), UV−vis spectroscopy, and fluorescent spectroscopy. Photocatalytic behavior of CuS/TiO_2 nanotubes was evaluated for photodecomposition of malachite green and phenol. The effect of CuS QDs was investigated by photobleaching of malachite green in a Ray-sorb reactor (optical filtration at wavelength <600 nm). The results suggest that CuS QDs can enhance photocatalytic activity and improve photosensitivity of the TiO_2 nanotubes using visible light.

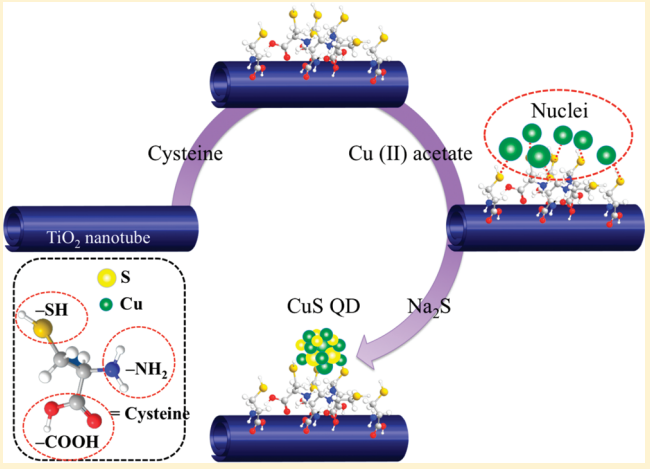

INTRODUCTION

The photocatalytic properties of TiO_2 have been exploited in various applications including solar conversion[1−3] and environmental detoxification,[4,5] as well as biomedical applications.[6−9] TiO_2 nanostructures such as nanoparticles, nanorods, nanofibers, and nanotubes have been shown to have a higher catalytic activity compared to bulk TiO_2.[10,11] Multiwall TiO_2 nanotubes (TNTs), prepared by hydrothermal synthesis, are particularly interesting due to the large surface area. Unfortunately, the various forms of TiO_2 are wide band gap semiconductors. Therefore, one needs to modify the band gap of TNTs, reported to be in a range of 3.3−3.87 eV,[12,13] or to add a sensitizer to adsorb light in the visible or near IR region of the solar spectrum. We have previously reported the preparation of lead sulfide (PbS) quantum dots on TiO_2 nanotubes[14] and the photocatalytic degradation of organic dyes using >600 nm light.[4] Since lead presents potential environmental and health problems, we have examined more eco-friendly quantum dots. The copper sulfides (Cu_xS), which are *p*-type semiconducting materials, caused by copper vacancies within the lattice, are of particular interest. There are five stable Cu_xS ($1 \le x \le 2$) phases: covellite (CuS) in the copper-deficient region and anlilite ($Cu_{1.75}S$), digenite ($Cu_{1.8}S$), djurleite ($Cu_{1.95}S$), and chalcocite (Cu_2S) in the copper-rich region.[15−18] The band gap of Cu_xS is dependent on the average oxidation state of Cu (E_g = 1.2, 1.5, and 2.0 eV for Cu_2S, $Cu_{1.8}S$, and CuS, respectively).[19] There is growing interest in these phases for solar cells, solar controllers, nonlinear materials, lithium-ion batteries, gas sensors, and catalysts.[20−24] The green copper sulfide (CuS) covellite is attractive since it has an additional absorption band in the NIR.[19,22,25] Moreover, CuS maintains transmittance in the infrared and exhibits low reflectance in the visible and relatively high reflectance in the near-infrared region, which makes it a prime candidate for solar energy adsorption.[26]

Herein, we describe the synthesis of CuS quantum dots (CuS QDs) onto the surface of TiO_2 nanotubes at room temperature. The deposition of CuS QDs on both the inside and outside of TNTs was accomplished by using cysteine linkers. The formation of the CuS/TNTs was followed by FT-IR spectroscopy after each deposition step. The morphologies, phase, and optical properties of as-synthesized materials were studied using TEM, XRD, UV−vis spectroscopy, and photoluminescence spectroscopy. The photocatalytic behavior of the CuS/TNTs and the effect of CuS QDs were evaluated for the photodegradation of malachite green and phenol at different wavelengths.

EXPERIMENTAL SECTION

Materials. P25 TiO_2 nanoparticles (80% anatase and 20% rutile) were obtained from Evonik (Degussa Corp). L-Cysteine (≥97%), copper(II) acetate, sodium sulfide nonahydrate (<98%, ACS reagent), and sodium hydroxide (97%, ACS reagent, pellets) were purchased from Sigma-Aldrich. Malachite green

Received: October 10, 2010
Revised: March 6, 2011

 © XXXX American Chemical Society dx.doi.org/10.1021/jp109716q | *J. Phys. Chem. C* XXXX, XXX, 000–000

and phenol were purchased from Alfa Aesar. All chemicals were used without further purification.

Preparation of TNTs. The TNTs were synthesized using a literature procedure.[27] A mixture of 0.5 g of P25 nanoparticles and 30 mL of a 10 M NaOH aqueous solution was stirred at room temperature for 10 min. The mixture was then transferred to a Teflon-lined autoclave and heated at 150 °C for 24 h. The resulting white precipitate was stirred in 250 mL of 0.1 M HCl overnight followed by washing with DI water until a pH of 7 was achieved. The TNT product was then dried at 90 °C for 12 h followed by annealing at 350 °C for 75 min.

Fabrication of CuS/TNTs. An amount of 0.25 g of TNTs was treated with 25 mL of a 0.3 M L-cysteine aqueous solution and adjusted to pH 4 with a 0.1 M HCl solution. The mixture then was kept in the dark for an hour at RT without stirring. The pretreated TNTs were washed with DI water to remove unattached cysteine, filtered, and dried at 50 °C. A 0.1 M Cu(II) acetate aqueous solution was added to the cysteine coated TNTs which were stored in the dark for 15 min then washed with DI water followed by drying at 50 °C for 10 h. The TNTs were reacted with 0.3 M Na_2S at RT to form the CuS/TNTs.

Characterization. FT-IR spectra were collected on a Perkin-Elmer GX FT-IR spectrometer from KBr pellets as the sample matrix. X-ray powder diffraction (XRD) patterns were recorded using a Riguku Ultima III X-ray diffractometer with Cu Kα radiation. The microstructures of CuS/TNTs was studied by transmission electron microscopy (TEM) using a FEI CM200 FEG transmission electron microscope operating at 200 kV. The size distribution of CuS QDs was calculated from the TEM images of 300 nanoparticles. The UV/vis/near-IR diffuse reflectance spectra were collected on a Perkin-Elmer Lambda 900 UV−vis/NIR spectrophotometer. Fluorescence spectra were obtained using a Perkin-Elmer LS55 Fluorimeter.

Photocatalytic Activity of CuS/TNTs. The photodegradation of malachite green and phenol was used to evaluate the photocatalytic activity of the CuS/TNTs catalyst. Malachite green (0.3 mM) (in DI water) was prepared (initial pH = 6.2). The photocatalysis experiment was set up in a dark cabinet to isolate a high intensity light source. A water-cooled 450 W Hanovia quartz mercury lamp was placed 15 cm from the reactor. Three different reactors were used in this experiment: quartz, Pyrex, and Ray-sorb reactors. A mixture of 25 mg of catalyst and 100 mL of a 0.3 mM malachite green aqueous solution was loaded into a reactor and stirred in the dark at RT for 30 min to allow the complete equilibration of the adsorption/desorption of substrate on the catalyst. At various time intervals, 5 mL aliquots from the reaction were sampled and centrifuged to remove the catalyst particles. The UV−vis spectra of the supernatant were recorded (at λ = 617 nm) to determine the concentration of residual dye in the reaction. Three sets of data were collected for each experimental condition. Photodegradation of phenol was tested under the same procedure.

A stability test of CuS/TNTs in both quartz and Ray-sorb reactor was evaluated by using the photodegradation of malachite green as a model reaction. Malachite green was catalyzed for 4 h, and then the catalyst was recovered (by centrifugation) and washed with DI water. A new batch of malachite green solution was added to the reactor containing the recovered catalyst. The CuS/TNT catalyst was reused for three cycles to probe the catalyst stability.

RESULTS AND DISCUSSIONS

Formation of CuS/TNTs. The synthesis pathway of the CuS/TNTs is shown in Scheme 1 which is similar to that previously reported by us for the preparation of PbS quantum dots on TNTs.[4,14] To anchor and control the size of the CuS QDs on the TNTs, L-cysteine was used as a linker. L-Cysteine is an amino acid that contains three reactive centers: a thiol group (−SH), an amine ($-NH_2$), and a carboxylic acid (−COOH) which could assist in binding the CuS nanocrystals to the surface of TiO_2. To prevent the formation of bulk CuS, the TNTs were first treated with cysteine which provides a binding site for copper ions (step 1 of Scheme 1). After adding a copper(II) acetate solution, the Cu(II) ions, which were expected to have a high affinity for the thiol group, readily reacted with cysteine molecules as evidenced by a deep blue-green color, indicating the formation of Cu(II)−cysteine complexes (step 2 of Scheme 1). CuS nanocrystals were then grown after adding a Na_2S solution. The formation of CuS QDs on the TNTs was followed using FT-IR spectroscopy. The FT-IR spectra of pure TNTs, cysteine, and the products after each deposition step are shown in Figure 1. The FT-IR spectrum of the pure TNTs (Figure 1a) reveals only the broad shoulder to the Ti−O stretching mode below

Scheme 1. Fabrication of CuS QD Doped TiO_2 Nanotubes

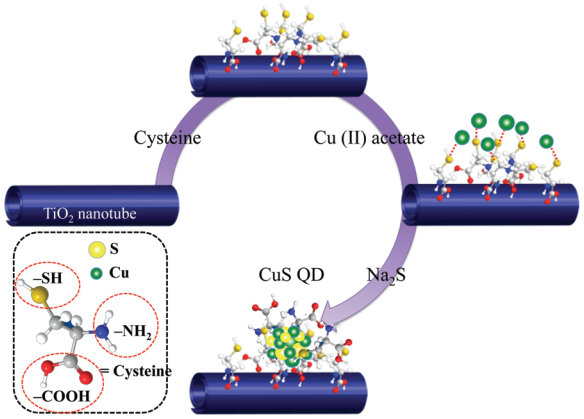

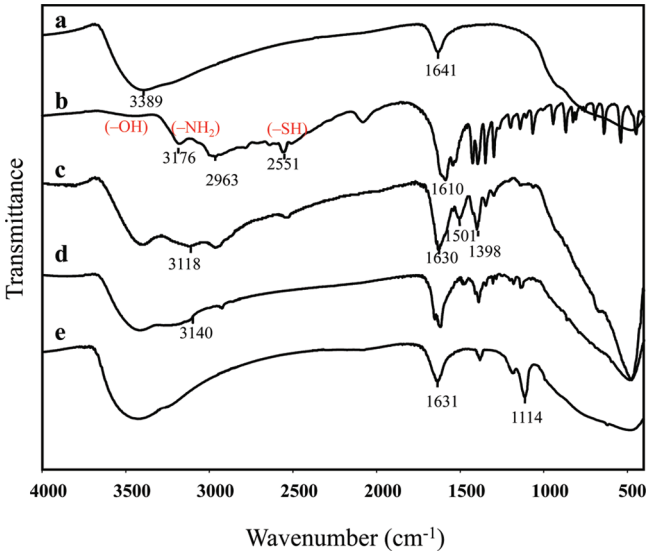

Figure 1. FT-IR spectra of (a) TNTs, (b) cysteine, (c) pretreated TNTs (with cysteine), (d) pretreated TNTs followed by absorption of Cu^{2+}, and (e) CuS/TNTs.

dx.doi.org/10.1021/jp109716q |J. Phys. Chem. C XXXX, XXX, 000–000

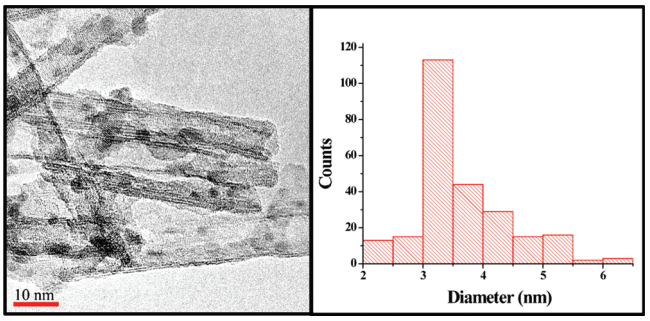

Figure 2. TEM image of CuS QD doped TiO_2 nanotubes and the corresponding size distribution of CuS QDs.

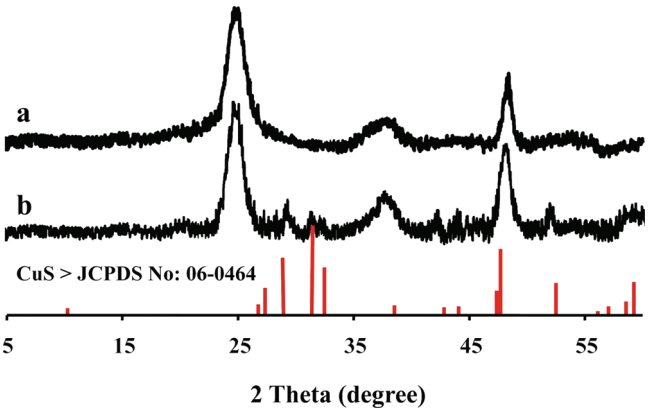

Figure 3. XRD patterns: (a) TiO_2 nanotubes and (b) CuS QD doped TNTs.

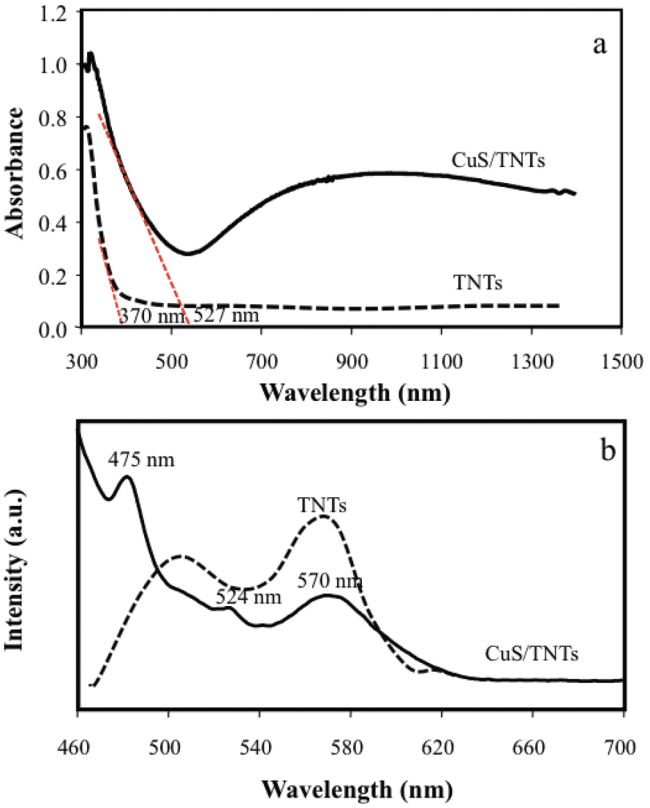

Figure 4. Optical properties of CuS/TNTs: (a) UV−vis spectra of CuS/TNTs and TNTs and (b) photoluminescence emission spectra of CuS/TNTs and TNTs.

1000 cm^{-1} as well as adsorbed water. The peaks at 3389 and 1641 cm^{-1} can be assigned to O−H stretching and the H−O−H bending mode.[14,28] The FT-IR spectrum of pure cysteine is shown in Figure 1b. The peaks at 3176, 2963, and 2551 cm^{-1} have been assigned to the vibration frequencies of the $-NH_3^+$, $-CH_2$, and −SH groups. Moreover, the deformation frequencies of the NH_3^+ group can be found in the 1640−1610 cm^{-1} region.[29,30] The peak at 1610 cm^{-1} is characteristic of an antisymmetric stretching vibration of the COO^- group in cysteine (zwitterion form: $H_3N^+-R-COO^-$). Absorption of cysteine on the surface of the TNTs is likely via the carboxylate group which is consistent with a decrease of the band at ~1200 cm^{-1} (−CO) and the increase of the bands at 1501 and 1389 cm^{-1} (antisymmetric and symmetric vibrations of the carboxylate salt).[31] The FT-IR spectrum of the pretreated TNTs after adding copper ions (Figure 1c) shows a disappearance of the −SH band at 2551 cm^{-1}, consistent with the binding of Cu^{2+} ions to the thiol groups. The CuS nanoparticles were formed after adding a Na_2S solution, but the resulting FT-IR spectrum of the CuS/TNTs is very broad (Figure 1d). The bands assigned to the vibrational modes of cysteine are not as strong as in Figure 1c which suggests that some of the cysteine may be lost during formation of the CuS nanoparticles. The peak at 1114 cm^{-1} is characteristic of an S−O stretch which suggests partial oxidation of the CuS; however, there is no evidence of crystalline sulfate, thiosulfate, or oxide phases (vide infra).

Morphologies and Crystal Structure. As shown in the TEM image in Figure 2, the CuS nanocrystals only grow on the surface of the TNTs, and there is no evidence of bulk CuS or unattached CuS QDs. The CuS QDs appear on both the inside and outside TNT surfaces. The corresponding size distribution indicates that CuS QDs with an average size of 3.6 ± 0.4 nm were made. A comparison of XRD patterns of TNTs and CuS/TNTs is shown in Figure 3a and 3b, respectively. The XRD pattern for the TNTs corresponds to the anatase phase,[14] whereas the XRD pattern of CuS/TNTs shows additional reflections which appear to match with the reported hexagonal CuS phase (JCPD card No. 06.0464). The other Cu_xS phases or potential byproducts such as CuO, Cu_2O, and $CuSO_4$ exhibit distinctly different X-ray patterns that do not match any of the reflections in Figure 3b. The size of the CuS QDs calculated using the Scherrer equation was 3.9 nm, which is in close agreement with the TEM results.

Optical Properties of CuS/TNTs. The as-synthesized CuS/TNTs are a uniform green color. The UV−vis spectrum of the CuS/TNTs (Figure 4a) shows an absorption band with a maximum wavelength near 320 nm and a broad band in the near-IR region. The optical band gap energy (E_g) of CuS QDs was measured to be 2.35 eV (527 nm) which is larger than the reported value for bulk CuS (2.0 eV)[16,19] owing to a quantum size effect, whereas the band gap energy of the TNTs was calculated to be 3.35 eV (370 nm). The near-IR band of the CuS has been investigated by many researchers. One explanation is that the near-IR band arises from charge transfer from a CuS core to an oxidized $CuS_{(ox)}$ shell, which occurs when heating the sample in oxygen.[32,33] Raevskaya and co-workers also reported that surface oxidation of Cu_xS nanoparticles generated the chromophoric centers, which are corresponding to mixed-valence copper (I, II) which results in an intervalence charge transfer absorption band in the near-IR region.[34] Brelle et al. proposed an

dx.doi.org/10.1021/jp109716q |J. Phys. Chem. C XXXX, XXX, 000–000

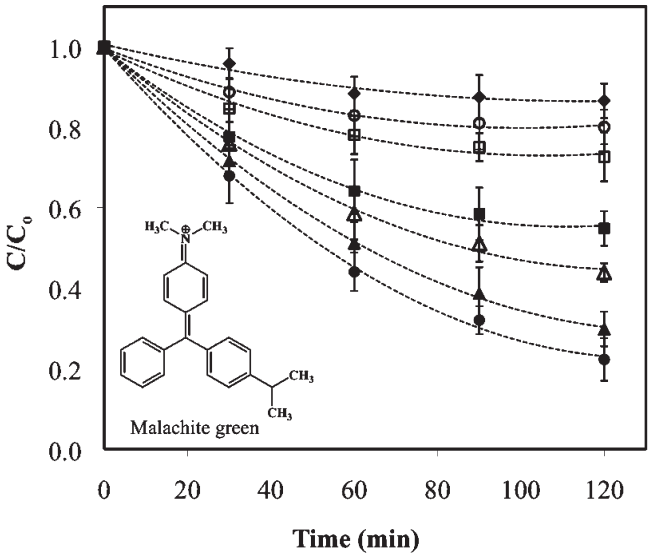

Figure 5. Plot of dye concentration versus irradiation time for the photodegradation of malachite green catalyzed by TNTs (△) and CuS/TNTs (▲) in the quartz reactor, TNTs (□) and CuS/TNTs (■) in the Pyrex reactor, TNTs (○) and CuS/TNTs (●) in the Ray-sorb reactor, and the blank without catalyst (♦).

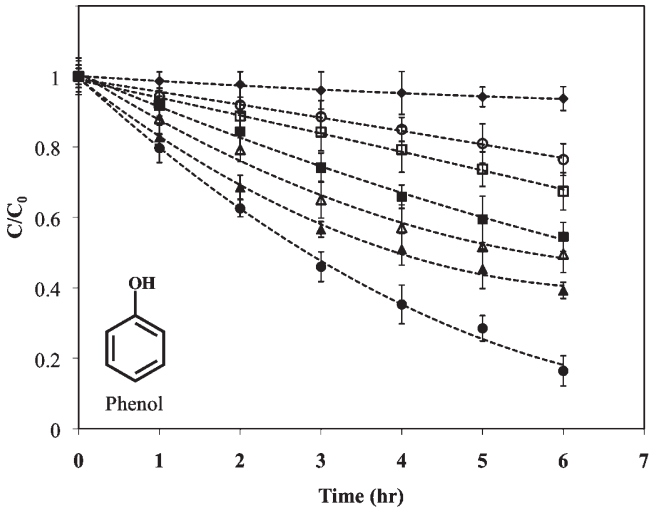

Figure 6. Plot of dye concentration versus irradiation time for the photodegradation of phenol catalyzed by TNTs (△) and CuS/TNTs (▲) in the quartz reactor, TNTs (□) and CuS/TNTs (■) in the Pyrex reactor, TNTs (○) and CuS/TNTs (●) in the Ray-sorb reactor, and the blank without catalyst (♦).

energy level diagram for CuS, which involves the generation of midgap states due to surface oxidation, and the near IR band is then transitioned from the midgap state to the conduction band.[25] The FT-IR spectrum of as-synthesized CuS/TNTs (Figure 1d) shows a band at 1114 cm^{-1}, consistent with the S−O stretch for thiosulfate. Since there is no XRD evidence for oxidation products, this is likely limited to the QD surface. Dunn and Muzenda studied the thermal oxidation of covellite (CuS). They reported that no oxides or sulfates were detected up to 330 °C.[35] Since the only detectable diffraction pattern comes from CuS, the structure of the QDs should largely be CuS with maybe a thin layer of oxidized CuS.

The photoluminescence emission spectrum of CuS/TNTs is shown in Figure 4b. Three emission peaks were observed at 475, 524, and 570 nm. The emission at 570 nm was assigned to the TiO_2 nanotubes. Qian and co-workers reported that the titania nanotubes are composed of the Ti−OH complexes which can act as a luminescent center, yielding the emission peak at ∼582 nm when the nanotubes were annealed at 300 °C.[36] The bands at 475 and 524 nm are consistent with the results reported for CuS.[15,37−41]

Photocatalytic Activity of TiO_2 Nanotubes Decorated with CuS QDs. In this study, three different reactors, including quartz, Pyrex (optical filtration at wavelength <310 nm), and Ray-sorb (optical filtration at wavelength <600 nm) were used to test the photocatalytic activity of the CuS/TNTs. The photodegradation of malachite green was used as a model reaction to compare the activities of the TNTs and the CuS/TNTs. A plot of malachite green concentration versus irradiation time is shown in Figure 5. There are several reports of CuS as a photocatalyst. For example, Li et al. showed that CuS nanomaterials with hierarchical structures could be used for photodecomposition of methylene blue.[40] CuS nanoflowers were reported to be better photocatalysts for degradation of rhodamine B than Degussa P25 (TiO_2 nanoparticles).[42,43] The photocatalytic improvement of the CuS/TNTs relative to pure TNTs could arise from CuS QDs functioning as a cocatalyst. Moreover, coupling CuS nanoparticles with the TNTs may prevent electron−hole recombination. For photodecomposition of organic compounds to occur, the photocatalysts must absorb light and generate excitons, as well as adsorb the substrate on the catalytic surface. Since the lifetime and diffusion distance of most reactive oxygen species (ROS), such as superoxide, peroxide, singlet oxygen, and hydroxyl radicals, are short[44] the reactants need to be adsorbed on the surface of the CuS/TNTs catalysts. So, the photooxidation of malachite green could depend on the interaction of dye with the TNT surface. The malachite green is a cationic dye which readily binds to the negatively charged surface of TNTs at pH > 3.[45] In the case of the TNTs, the relative catalytic activities in the different reactors are quartz > Pyrex > Ray-sorb. Since the Pyrex and the Ray-sorb filter the UV light absorbed by the TNTs (an exciton absorption around 366 nm), there was minimal photodegradation of the dye. Some of the loss of dye from solution in this case is simply from adsorption on the TNTs. For the CuS/TNT catalysts, the relative catalytic activities in the different reactors are Ray-sorb > quartz > Pyrex. The photodegradation of malachite green on CuS/TNTs dropped upon changing from the quartz reactor to the Pyrex, but the activity is greater than for the TNTs alone. Surprisingly, photobleaching of malachite green on CuS/TNTs in the Ray-sorb reactor was greater than for reaction in a quartz reactor. One possible reason is that when using the full spectrum available from the halogen lamp in the quartz reactor malachite green undergoes decomposition to intermediates including phenols[46] that might interfere with the adsorption of dye on the TNT surface. A comparison of the photocatalytic activities of TNTs and CuS/TNTs in the Ray-sorb shows that only CuS/TNTs can catalyze the photobleaching of malachite green. Because the CuS QDs can absorb the filtered light (>600 nm), energy transfer from CuS QDs can promote the generation of ROS on TNTs.

Results for the photodegradation of phenol are shown in Figure 6. The photocatalytic activity of the CuS/TNTs was higher than that of TNTs, in the quartz, Ray-sorb, and Pyrex reactors. Moreover, a similar catalytic behavior of CuS/TNTs was observed for photodecomposition of phenol and malachite

dx.doi.org/10.1021/jp109716q |J. Phys. Chem. C XXXX, XXX, 000–000

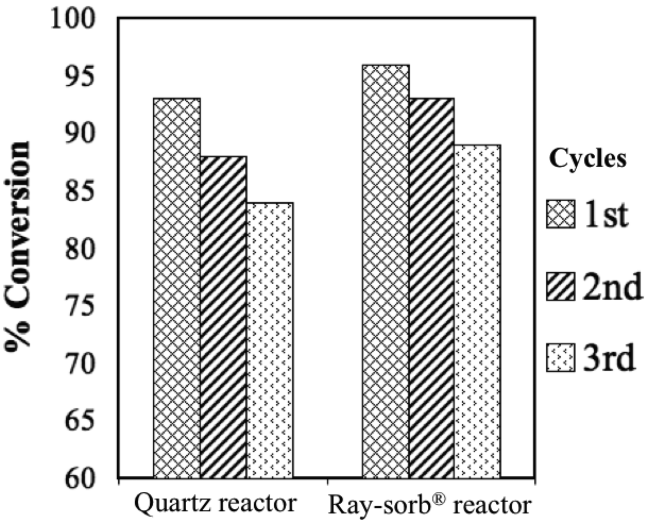

Figure 7. Plot of % conversion for the photodegradation of malachite green catalyzed CuS/TNTs in the quartz reactor and Ray-sorb reactor.

green where the relative rates of decomposition in the different reactors were Ray-sorb > quartz > Pyrex. The mid gap states of the CuS QDs which may help prevent recombination appear to be important in understanding this unexpected result and merits further study.

The stability of the CuS/TNTs was evlauated using the photodegradation of malachite green as a model reaction. A plot of % conversion as a function of the number of cycles for the photodegradation of malachite green in the quartz and Ray-sorb reactors is shown in Figure 7. The conversion of dye was calculated after 4 h of irradiation. The decreases in percent conversion after recycling the catalyst for 3 cycles were found to be 9.7% and 7.3% in quartz and Ray-sorb reactors, respectively. The drop in activity after reusing the catalyst could be associated to the loss of catalyst during the recovering process and catalyst poisoning. The results confirm that CuS/TNTs are practical catalysts for photodecomposion of organic pollutants. These catalysts are also stable under the reaction conditions.

CONCLUSION

For the first time, we have demonstrated a simple method to deposite CuS QDs onto the surface of TiO_2 nanotubes at room temperature. The CuS QDs 3−4 nm in diameter were attached to the TNTs in the controlled manner by using cysteine linkers. The optical properties of CuS doped TiO_2 nanotubes show an improved photoresponse in the visible and near-IR regions. The photoactivity of the CuS/TNTs was maintained even when irradiated at wavelengths longer than the exciton absorption of the TiO_2 nanotubes. These results suggest that CuS QDs can be utilized as a cocatalyst to expand the usable light absorption of the TNTs.

AUTHOR INFORMATION

Corresponding Author

*E-mail: balkus@utdallas.edu.

ACKNOWLEDGMENT

This work was supported by the National Science Foundation grant No. CBET-0854059.

REFERENCES

(1) Chong, L. W.; Chien, H. T.; Lee, Y. L. *J. Power Sources* **2010**, *195*, 5109.
(2) Ganapathy, V.; Karunagaran, B.; Rhee, S. W. *J. Power Sources* **2010**, *195*, 5138.
(3) Lee, Y.; Kang, M. *Mater. Chem. Phys.* **2010**, *122*, 284.
(4) Ratanatawanate, C.; Tao, Y.; Balkus, K. J., Jr *J. Phys. Chem. C* **2009**, *113*, 10755.
(5) Taoda, H. *Res. Chem. Intermed.* **2008**, *34*, 417.
(6) Xu, J.; Sun, Y.; Huang, J.; Chen, C.; Liu, G.; Jiang, Y.; Zhao, Y.; Jiang, Z. *Bioelectrochemistry* **2007**, *71*, 217.
(7) Janczyk, A.; Wolnicka-lubisz, A.; Urbanska, K.; Kisch, H.; Stochel, G.; Macyk, W. *Free Radical Biol. Med.* **2008**, *44*, 1120.
(8) Lei, W.; Zhou, Q.; Li, Z.; Wang, X.; Zhang, B. *Chem. Lett.* **2009**, *38*, 1138.
(9) Jiang, G.; Zeng, J. *J. Appl. Polym. Sci.* **2010**, *116*, 779.
(10) Chatterjee, S.; Bhattacharyya, K.; Ayyub, P.; Tyagi, A. K. *J. Phys. Chem. C* **2010**, *114*, 9424.
(11) Hsieh, W. P.; Pan, J. R.; Huang, C.; Su, Y. C.; Juang, Y. J. *Sci. Total Environ.* **2010**, *408*, 672.
(12) Jiang, Z.; Yang, F.; Luo, N.; Chu, B. T. T.; Sun, D.; Shi, H.; Xiao, T.; Edwards, P. P. *Chem. Commun.* **2008**, 6372.
(13) Bavykin, D. V.; Gordeev, S. N.; Moskalenko, A. V.; Lapkin, A. A.; Walsh, F. C. *J. Phys. Chem. B* **2005**, *109*, 8565.
(14) Ratanatawanate, C.; Xiong, C.; Balkus, K. J., Jr *ACS Nano* **2008**, *2*, 1682.
(15) Chen, G. Y.; Deng, B.; Cai, G. B.; Dong, W. F.; Zhang, W. X.; Xu, A. W. *Cryst. Growth Des.* **2008**, *8*, 2137.
(16) Kuzuya, T.; Itoh, K.; Ichidate, M.; Wakamatsu, T.; Fukunaka, Y.; Sumiyama, K. *Electrochim. Acta* **2007**, *53*, 213.
(17) Shan, J.; Pulkkinen, P.; Vainio, U.; Maijala, J.; Merta, J.; Jiang, H.; Serimaa, R.; Kauppinen, E.; Tenhu, H. *J. Mater. Chem.* **2008**, *18*, 3200.
(18) Cheng, G.; Hight Walker, A. R. *Anal. Bioanal. Chem.* **2010**, *396*, 1057.
(19) Zhao, Y.; Pan, H.; Lou, Y.; Qiu, X.; Zhu, J.; Burda, C. *J. Am. Chem. Soc.* **2009**, *131*, 4253.
(20) Page, M.; Niitsoo, O.; Itzhaik, Y.; Cahen, D.; Hodes, G. *Energy Environ. Sci.* **2009**, *2*, 220.
(21) Isac, L.; Duta, A.; Kriza, A.; Manolache, S.; Nanu, M. *Thin Solid Films* **2007**, *515*, 5755.
(22) Wang, K. J.; Li, G. D.; Li, J. X.; Wang, Q.; Chen, J. S. *Cryst. Growth Des.* **2007**, *7*, 2265.
(23) Roy, P.; Srivastava, S. K. *Cryst. Growth Des.* **2006**, *6*, 1921.
(24) Sagade, A. A.; Sharma, R. *Sens. Actuators, B* **2008**, *133*, 135.
(25) Brelle, M. C.; Torres-Martinez, C. L.; McNulty, J. C.; Mehra, R. K.; Zhang, J. Z. *Pure Appl. Chem.* **2000**, *72*, 101.
(26) Zhang, F.; Wong, S. S. *Chem. Mater.* **2009**, *21*, 4541.
(27) Kasuga, T.; Hiramatsu, M.; Hoson, A.; Sekino, T.; Niihara, K. *Langmuir* **1998**, *14*, 3160.
(28) Bavykin, D. V.; Friedrich, J. M.; Walsh, F. C. *Adv. Mater.* **2006**, *18*, 2807.
(29) Brigatti, M. F.; Lugli, C.; Montorsi, S.; Poppi, L. *Clays Clay Miner.* **1999**, *47*, 664.
(30) Dokken, K. M.; Parsons, J. G.; McClure, J.; Gardea-Torresdey, J. L. *Inorg. Chim. Acta* **2009**, *362*, 395.
(31) Rajh, T.; Ostafin, A. E.; Micic, O. I.; TieÃÄde, D. M.; Thurnauer, M. C. *J. Phys. Chem.* **1996**, *100*, 4538.
(32) Yumashev, K. V.; Malyarevich, A. M.; Prokoshin, P. V.; Artem'ev, M. V.; Gurin, V. S.; Mikhailov, V. P. *Quantum Electron.* **1997**, *27*, 722.
(33) Artemyev, M. V.; Gurin, V. S.; Yumashev, K. V.; Prokoshin, P. V.; Maljarevich, A. M. *J. Appl. Phys.* **1996**, *80*, 7028.
(34) Raevskaya, A. E.; Stroyuk, A. L.; Kuchmii, S. Y.; Kryukov, A. I. *J. Mol. Catal. A: Chem.* **2004**, *212*, 259.
(35) Dunn, J. G.; Muzenda, C. *Thermochim. Acta* **2001**, *369*, 117.
(36) Qian, L.; Jin, Z. S.; Yang, S. Y.; Du, Z. L.; Xu, X. R. *Chem. Mater.* **2005**, *17*, 5334.

(37) Li, F.; Bi, W.; Kong, T.; Qin, Q. *Cryst. Res. Technol.* **2009**, *44*, 729.
(38) Xu, K.; Ding, W. *Mater. Lett.* **2008**, *62*, 4437.
(39) Kalyanikutty, K. P.; Nikhila, M.; Maitra, U.; Rao, C. N. R. *Chem. Phys. Lett.* **2006**, *432*, 190.
(40) Li, F.; Wu, J.; Qin, Q.; Li, Z.; Huang, X. *Powder Technol.* **2010**, *198*, 267.
(41) Li, F.; Kong, T.; Bi, W.; Li, D.; Li, Z.; Huang, X. *Appl. Surf. Sci.* **2009**, *255*, 6285.
(42) Ding, T. Y.; Wang, M. S.; Guo, S. P.; Guo, G. C.; Huang, J. S. *Mater. Lett.* **2008**, *62*, 4529.
(43) Cheng, Z.; Wang, S.; Wang, Q.; Geng, B. *CrystEngComm.* **2009**, *12*, 144.
(44) Ishibashi, K. I.; Nosaka, Y.; Hashimoto, K.; Fujishima, A. *J. Phys. Chem. B* **1998**, *102*, 2117.
(45) Bavykin, D. V.; Milsom, E. V.; Marken, F.; Kim, D. H.; Marsh, D. H.; Riley, D. J.; Walsh, F. C.; El-Abiary, K. H.; Lapkin, A. A. *Electrochem. Commun.* **2005**, *7*, 1050.
(46) Vinu, R.; Akki, S. U.; Madras, G. *J. Hazard. Mater.* **2010**, *176*, 765.